How to cite: *Angew. Chem. Int. Ed.* **2024**, *63*, e202401433
doi.org/10.1002/anie.202401433

Chelotropic Rearrangements

Ynamide and Azaalleneyl. Acid-Base Promoted Chelotropic and Spin-State Rearrangements in a Versatile Heterocumulene $[(Ad)NCC(^tBu)]^-$

John B. Russell, Mehrafshan G. Jafari, Jun-Hyeong Kim, Bimal Pudasaini, Andrew Ozarowski, Joshua Telser, Mu-Hyun Baik, and Daniel J. Mindiola**

Abstract: We introduce the heterocumulene ligand $[(Ad)NCC(^tBu)]^-$ (Ad = 1-adamantyl ($C_{10}H_{15}$), ^tBu = *tert*-butyl, (C_4H_9)), which can adopt two forms, the azaalleneyl and ynamide. This ligand platform can undergo a reversible chelotropic shift using Brønsted acid-base chemistry, which promotes an unprecedented spin-state change of the $[V^{III}]$ ion. These unique scaffolds are prepared via addition of 1-adamantyl isonitrile (C≡NAd) across the alkylidyne in complexes $[(BDI)V{\equiv}C^tBu(OTf)]$ (**A**) (BDI^-=ArNC(CH_3)CHC(CH_3)NAr), Ar = 2,6-$^iPr_2C_6H_3$) and $[(dBDI)V{\equiv}C^tBu(OEt_2)]$ (**B**) ($dBDI^{2-}$=ArNC(CH_3)CHC(CH_2)NAr). Complex **A** reacts with C≡NAd, to generate the high-spin $[V^{III}]$ complex with a κ^1-*N*-ynamide ligand, $[(BDI)V\{\kappa^1\text{-}N\text{-}(Ad)NCC(^tBu)\}(OTf)]$ (**1**). Conversely, **B** reacts with C≡NAd to generate a low-spin $[V^{III}]$ diamagnetic complex having a chelated κ^2-*C*,*N*-azaalleneyl ligand, $[(dBDI)V\{\kappa^2\text{-}N,C\text{-}(Ad)NCC(^tBu)\}]$ (**2**). Theoretical studies have been applied to better understand the mechanism of formation of **2** and the electronic reconfiguration upon structural rearrangement by the alteration of ligand denticity between **1** and **2**.

Metallacyclobutadienes (MCBD, Scheme 1i) have been vital in the discovery and implementation of a plethora of organometallic reactions to form and break C–C and C–heteroatom multiple bonds. The most notable organometallic transformation that utilizes such four-membered

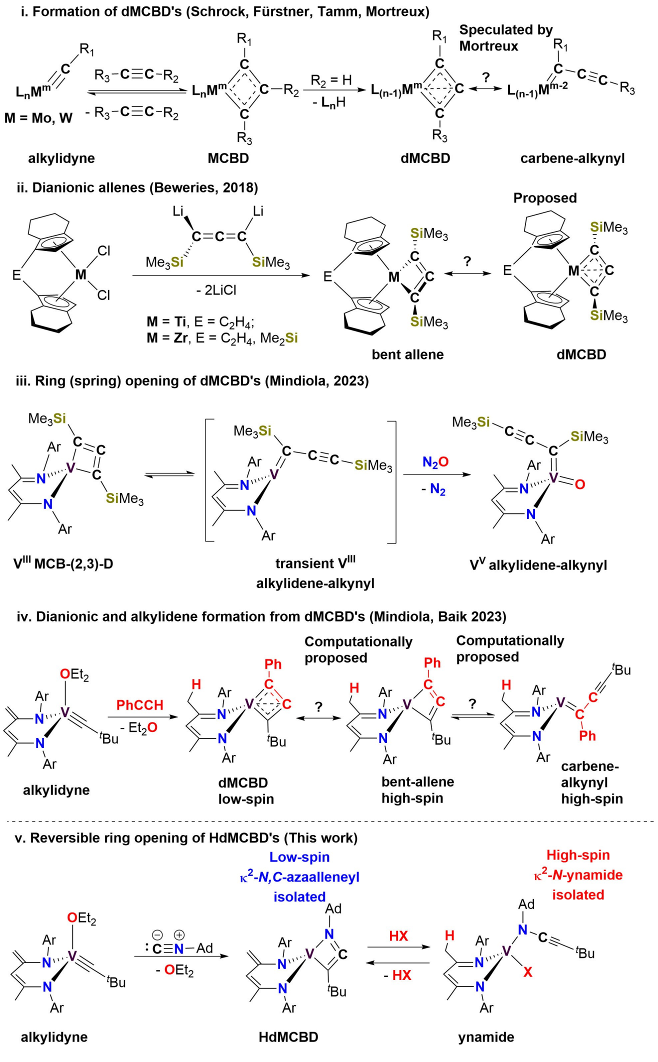

Scheme 1. Methods to access deprotiometallacyclobutadienes (dMCBDs) and similarity to a heteroatom deprotiometallacyclobutadiene (HdMCBD, this work).

---

[*] J. B. Russell, Dr. M. G. Jafari, Prof. Dr. D. J. Mindiola
Department of Chemistry, University of Pennsylvania, Philadelphia, Pennsylvania 19104, United States.
E-mail: mindiola@sas.upenn.edu

Dr. J.-H. Kim, Dr. B. Pudasaini, Prof. Dr. M.-H. Baik
Department of Chemistry, Korea Advanced Institute of Science and Technology (KAIST) & Center for Catalytic Hydrocarbon Functionalizations, Institute for Basic Science (IBS), Daejeon 34141, Republic of Korea
E-mail: mbaik2805@kaist.ac.kr

Dr. A. Ozarowski
National High Magnetic Field Laboratory, Florida State University, Tallahassee, Florida 32310, United States.

Prof. Dr. J. Telser
Department of Biological, Physical and Health Sciences, Roosevelt University, Chicago, Illinois 60605, United States.

metallacycle is alkyne metathesis[1–6] whereby carbyne fragments are exchanged with an internal alkyne resulting in a new metal alkylidyne (Scheme 1, i) and alkyne. Taking advantage of such transformation therefore allows for the construction of macrocyclic rings,[7] acetylenic polymers,[8] and diacetylenes.[9] In addition to the metathesis reaction, the β-position on the MCBD can be deprotonated to form a deprotiometallacyclobutadiene (dMCBD, Scheme 1, i) when a terminal alkyne is utilized rather than an internal alkyne.[10–19] Interestingly, dMCBD fragments have been speculated to ring-open and form carbene-alkynyls (Scheme 1, i),[20–21] which was likely responsible in the formation of polyalkynes in earlier experiments.[15,18,21–26] Although dMCBD are speculated to be an undesired scaffold in the cross-metathesis reaction, these scaffolds are intriguing since they could potentially resonate to dianionic bent-allenes (Scheme 1, ii) akin to what Beweries reported with the trimethylsilyl-substituted 1,3-dilithioallene.[27–28]

Recently, our group demonstrated that a vanadacyclobuta-(2,3)-diene can undergo a chelotropic rearrangement through a transient [V^{III}] alkylidene-alkynyl to form a [V^{V}] oxo alkylidene-alkynyl species (Scheme 1, iii).[29] In a subsequent paper we identified that a vanadium alkylidyne could react with phenylacetylene (HCCPh) to form a dMCBD, but also resonate to a bent-allene which was accompanied by a spin-state change. Computational studies suggested that the [V^{III}] bent allene would ring-open to a high-spin [V^{III}] carbene-alkynyl and that such species was likely responsible in the cyclic polymerization of HCCPh (Scheme 1, iv).[21] Realizing that a spin-state change accompanies a chelotropic rearrangement from dMCBD, a bent allene, and a carbene-alkynyl ligand, we decided to explore the chemistry of a structurally similar ligand such as an azaalleneyl, where one of the terminal CR groups was replaced with NR. Herein, we report a synthetic route to a hetero deprotiometallacyclobutadiene scaffold or HdMCBD, and demonstrate how this system can undergo chelotropic rearrangement from ynamide or azaalleneyl, specifically, a monodentate κ^1-*N*-ynamide to a bidentate κ^2-*N*,*C*-azaalleneyl and *vice versa* with the aid of Brønsted acid-base chemistry (Scheme 1, v). This geometric rearrangement is accompanied by a spin-state change of the [V^{III}] ion.

The reaction of $[(BDI)V{\equiv}C^tBu(OTf)]$ (**A**) with 1 equiv. of C≡NAd in pentane at −35 °C for 30 minutes led to a color change from dark green to burgundy. Crystallization of the product was performed by slow concentration of a pentane solution of the reaction mixture using toluene as the sorbent at −35 °C overnight, affording dark, burgundy-colored and plate-like crystals of the vanadium κ^1-*N*-ynamide $[(BDI)V\{\kappa^1\text{-}N\text{-}(Ad)NCC(^tBu)\}(OTf)]$ (**1**) in 91 % yield (Figure 1, top reaction). Complex **1** was structurally characterized using single crystal X-ray diffraction studies (sc-XRD) and revealed formation of a rare κ^1-*N*-ynamide fragment. Complex **1** crystallizes in the monoclinic space group *P*2(1)/c (Figure 1, bottom left), and the most salient feature in the solid-state structure is a four-coordinate [V^{III}] center with a monodentate ynamide ligand bound through the *N*-atom. The presence of the alkynyl group is clearly evident from the short C–C bond (C_{31}–C_{32}: 1.203(2) Å) when compared to the alkyne moiety of the molecular titanium-zinc[30] and the scandium[31] ynamide motifs (1.205(5) Å and 1.217(2) Å, respectively). The IR spectrum of **1** also exhibits the signature $\nu_{C\equiv C}$ stretch at 2189 cm^{-1} that is assigned to the $\nu_{C\equiv C}$ in the ynamide fragment (Figure S11), also in agreement with the few previously characterized ynamide motifs.[30]

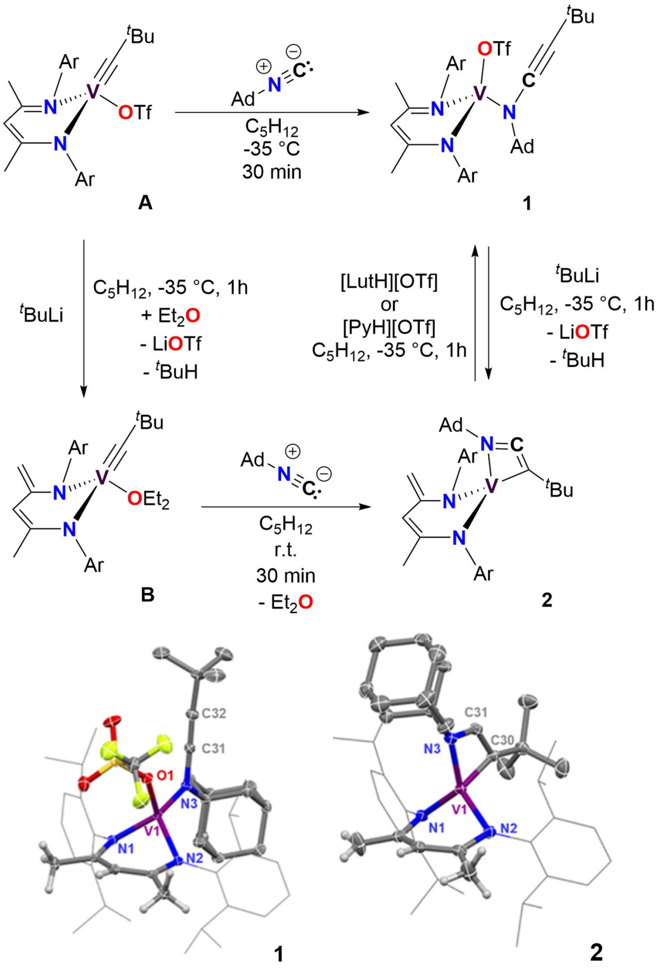

Figure 1. (Top) Reaction showing the synthesis of complexes **1** and **2** from reaction of C≡NAd with **A** and **B**, respectively, as well as their interconversion upon deprotonation and protonation of BDI$^-$ and dBDI^{2-} ligands, respectively, Ar = 2,6-^{i}Pr$_2$C$_6$H$_3$. (Bottom) Partial solid state ORTEP structures of **1** (bottom left) and **2** (bottom right) with 50 % probability ellipsoids. Hydrogen atoms and co-crystallized solvents are also omitted for clarity. Only hydrogens on the backbone of BDI$^-$ and dBDI^{2-} ligands relevant to the discussion are shown.

Complex **1** was confirmed to be a paramagnetic [V^{III}] species based on a solution Evans magnetic susceptibility study ($\mu_{eff} = 2.70\ \mu_B$ at 500 MHz, 300 K, benzene-d_6). This μ_{eff} value corresponds to an $S = 1$ with $g = 1.91$, which is reasonable for a less than half- filled (3d^2) configuration,[32] and is similar to the g_{iso} values derived from the g_{para} and g_{perp} values reported for $[V(H_2O)_6]^{3+}$ as a dopant in various diamagnetic single crystal hosts.[33] Given that **1** is a non-Kramers (i.e., integer spin) paramagnetic system, we also conducted high-frequency and high-field electron paramagnetic resonance (HFEPR) spectroscopic studies. The powder spectrum of compound **1** recorded at 10 K and 268 GHz

(Figure 2) reveals two distinct species, most likely conformers. Both species are highly rhombic $S = 1$ systems, which are indicative of low symmetry around the V^{III} ion (conformer **1-Δ**, $D = -1.785\ cm^{-1}$, $E = -0.575\ cm^{-1}$, $g_x = 1.948$, $g_y = 1.964$, and $g_z = 1.911$; conformer **1-Λ**, $D = +2.948\ cm^{-1}$, $E = +0.773\ cm^{-1}$, $g_x = 1.941$, $g_y = 1.943$, and $g_z = 1.978$, Figure 2). The magnitude of zfs in **1** is in line with that seen in other 4-coordinate [V^{III}] complexes such as those supported by pincer[34] and by β-diketiminate[35–36] ligands and with anionic monodentate C-,[34] N-,[35] and P-donor[36] ancillary ligands, i.e., ~1.5 $cm^{-1} < |D| \leq$ ~4 cm^{-1}.

Realizing that triflate can occupy a coordination site on the [V^{III}] metal center, we investigated whether changing the ancillary ligand on the vanadium alkylidyne would affect the denticity of the ynamide ligand in **1**. Thus, we probed the reactivity of C≡NAd with vanadium alkylidyne [(dBDI)V≡C^{t}Bu(OEt_2)] (**B**) ($dBDI^{2-}$=ArNC(CH_3)CHC(CH_2)NAr) since the anionic triflate ligand would be absent and the more labile etherate ligand would be prone to dissociate. Complex **B** is readily prepared from **A** via deprotonation with *tert*-butyl lithium (^{t}BuLi) in pentane at low-temperatures, followed by addition of diethyl ether (Et_2O) to the reaction mixture.[37] Accordingly, reaction of **B** with 1 equiv. of C≡NAd in most common hydrocarbon solvents resulted in an instantaneous color change from red to orange with formation of the κ^2-*C*,*N*-azaalleneyl [(dBDI)V{κ^2-*N*,*C*-(Ad)NCC(^{t}Bu)}] (**2**) in 91% isolated yield (Figure 1, bottom reaction) based on a combination of spectroscopic and structural studies. Akin to **1**, using a pentane/toluene vapor diffusion at −35 °C afforded single crystals of complex **2**, and sc-XRD revealed a unique coordination of the heterocumulene: A chelated κ^2-*C*,*N*-azaalleneyl binding mode (Figure 1, bottom right). Unlike **1**, however, the structure of **2** manifests C_1 symmetry due to the lack of a mirror plane in *bis*-anilido $dBDI^{2-}$ ligand. The most notable structural feature in **2** is the unprecedented chelating nature of the [(Ad)NCC(^{t}Bu)]$^-$ ligand, which results in essentially a bent azaalleneyl motif (∠N_3–C_{31}–C_{30} = 127.6(2)°), or arguably, a HdMCBD.

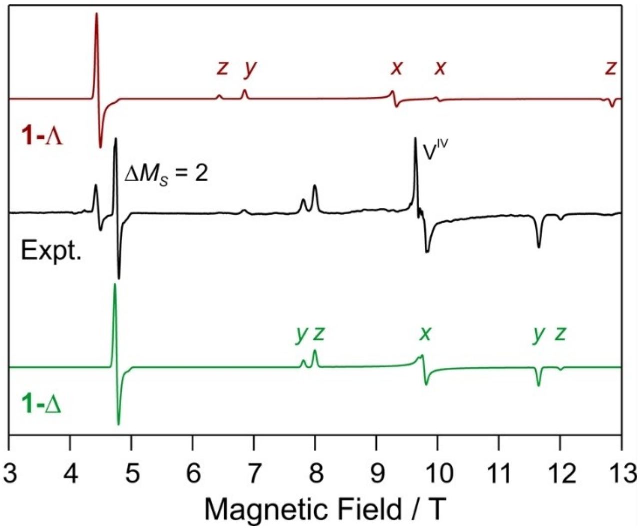

Figure 2. HFEPR spectrum of **1** collected at 10 K and 268 GHz (middle, black trace). The colored traces are simulations using spin Hamiltonian parameters (see text) of species **1-Δ** (top, red trace) and species **1-Λ** (bottom, green trace).

This bonding motif is in stark contrast to Xia's η^2- or η^1-iminoketenyl formed by 1,2-addition of the isonitrile across a cyclic and strained Os≡C bond (∠N–C–C = 169.8(3)°).[38] The structure of **2** also reveals relatively long V_1-N_3 and V_1-C_{30} distances of 1.877(1) and 1.843(2) Å, respectively, when compared to reported [V^{III}] complexes bearing V=N and V=C double bonds in examples such as CpV(NAr)(PMe_3)$_2$[39] and CpV(CH^{t}Bu)(dmpe)[40] (dmpe = 1,2-bis(dimethylphosphino)ethane) (1.698(2) and 1.809(3) Å, respectively). Moreover, the relatively short N_3-C_{31} and C_{31}-C_{30} distances of 1.331(2) and 1.394(2) Å, respectively, suggest this ligand scaffold to be best described as having canonical forms in the range of a bent azaalleneyl (Scheme 2, **2a**) and an η^2-azavinyl with a pendant imine donor (Scheme 2, **2b**). However, resonances such as **2c** and **2d** are also reasonable given that V_1-C_{30} and C_{31}-C_{30} have relatively short single bond lengths. The difference between resonance form **2a** and **2b** is the presence of a transannular V_1–C_{31} bond. In **2** the distance between V_1-C_{31} is 2.003(2)Å, which is comparable to previously characterized dMCBDs (1.967 Å–2.073 Å)[12,16, 19, 21, 29, 41–42] but noticeably shorter than the metallacyclobuta-(2,3)-diene complexes isolated by Reiß and Beweries (2.178 Å–2.284 Å).[43–44]

Taking advantage of the diamagnetism of complex **2**, we performed extensive multinuclear and multidimensional NMR spectroscopic experiments. In order to understand the chemical environment of the unsaturated β-carbon in the azaalleneyl ligand, we prepared ^{13}**C** isotopically enriched ^{13}**C**≡NAd (50% ^{13}**C**-enriched) via a bi-phasic reaction containing ^{13}**C**HCl_3 and adamantyl amine (H_2NAd).[45] Accordingly, the reaction of ^{13}**C**≡NAd with **B** under identical reaction conditions to making **2** forms the isotopologue [(dBDI)V{κ^2-*N*,*C*-(Ad)N^{13}**C**C(^{t}Bu)}] (**2-^{13}C**) and collecting its

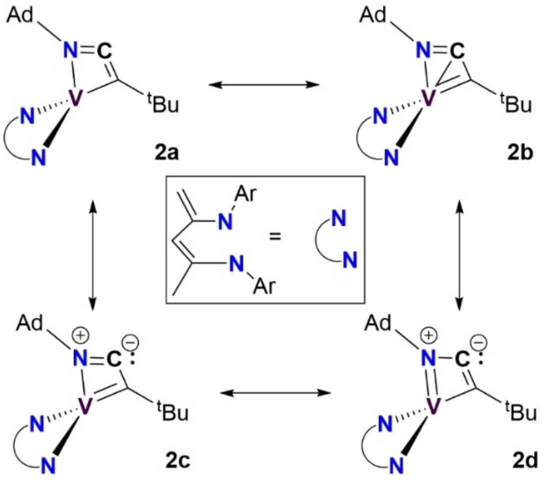

Scheme 2. Some possible resonance forms for complex **2**. Formal charges involving the nitrogen and vanadium atoms, and resonances having open-shell configurations have been excluded for clarity.

$^{13}C\{^1H\}$ NMR spectrum in benzene-d_6 reveals the intense and highly deshielded signal for β-carbon in the bent azaallenenyl at 226.78 ppm (Figure 3A). In contrast, the α-carbon in the same ligand scaffold resonates further upfield at 186.27 ppm. For comparison, in all carbon-based dMCBD complexes[11–12,14,16–17,19,21,41–44, 46–47] the α (164–233 ppm) and β (134–257 ppm) ^{13}C resonances are in good agreement with **2**. Complex **2** shows a broad single ^{51}V NMR resonance at 284 ppm ($\Delta\nu_{1/2} = 931$ Hz) (Figure S9) as well a single methine C*H* resonance at 5.78 ppm in ^1H NMR spectrum for the *bis*-anilido backbone. This ^1H signal correlates to a single carbon resonance at 98.27 ppm in ^1H–$^{13}C\{^1H\}$ HSQC NMR experiment (Figure 3B). These observations are all consistent with a single vanadium species present in solution.

Since **1** and **2** differ by the net presence of "HOTf" in the former we hypothesized that these species could interconvert using Brønsted acid-base chemistry and whether this strategy would allow for interconversion between a monodentate and chelate form. To our delight, complex **1** was found to transform to **2** by the slow addition of a cold pentane solution of ^{t}BuLi (1 equiv.), with concurrent loss of LiOTf (top of Figure 1). Conversely, the addition of one equivalent of a triflic acid source such as pyridinium triflate or lutidinium triflate to a cold solution of **2** leads to formation of **1**. The interconversion of **1** and **2** was confirmed by a combination of NMR spectroscopy and sc-XRD. Observing this transformation highlights the importance of the coordination environment of the heterocumulene ligand [(Ad)NCC(^{t}Bu)]$^-$ and its resemblance to the chelation effect of the bent allene scaffold (Scheme 1, i—iv).

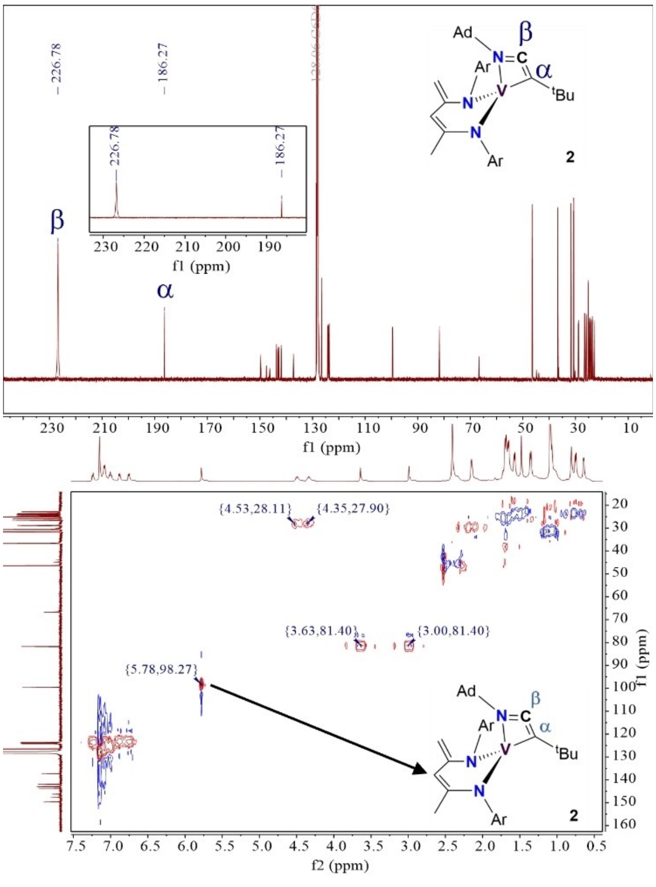

Figure 3. (A) $^{13}C\{^1H\}$ NMR spectrum of enriched **2-^{13}C**, with the inset of a zoomed in portion of the downfield region of the $^{13}C\{^1H\}$ NMR highlighting the β and α carbon resonances in **2-^{13}C** (126 MHz, benzene-d_6, 300 K) and (B) ^1H–$^{13}C\{^1H\}$ HSQC NMR spectrum of **2** ((500, 126) MHz, benzene-d_6, 300 K), benzene-d_6, 300 K).

To understand why the chelotropic rearrangement of the heterocumulene scaffold could affect the spin state of the [V^{III}] ion, we carried out density functional calculations at the B3LYP-D3/LACV3P/cc-pVTZ(-f)//LACVP/6-31G**[48–55] level of theory (see the Supporting Information for details). Our experimental findings on **2** suggested that its ground state adopts the low-spin configuration in a pseudo tetrahedral structure. Compared to the high-spin state of **1** supported by the BDI$^-$, we were curious how the dBDI^{2-} forces complex **2** to adopt the singlet low-spin ground state. A tetrahedral complex having two d-electrons such as **1** usually adopts a high-spin ground state by maximizing exchange stabilization through the energetically close d_{xy} and d_{xz} orbitals (Figure 4A). After releasing triflate, however, the empty coordination site on the vanadium allows for additional orbital interactions between the metal and the π*(C≡C) orbital of the [(Ad)NCC(^{t}Bu)]$^-$ moiety. This interaction results in a bonding interaction with the d_{xz} orbital, leading to a larger energy gap between those two d-orbitals. Thus, pairing two electrons in the lower-lying d_{xz} orbital becomes energetically more favorable than adopting the triplet state. Consistent with this rationale, DFT calculations on **2** predicted the d_{xz} and d_{xy} orbitals being the HOMO-1 and LUMO+1, respectively (Figure 4B). In addition, the HOMO-1 depicts a transannular bond between V_1 and the β-carbon atom of the NCC chelate, C_{31}. The appearance of a transannular bond was further supported by the Mulliken bond order index which was calculated to be 0.80 for the transannular bond. However, a QTAIM analysis (Figure S21) was conducted on **2** which suggested no bond path and critical points corresponding a transannular V–C bond. With this ambiguous

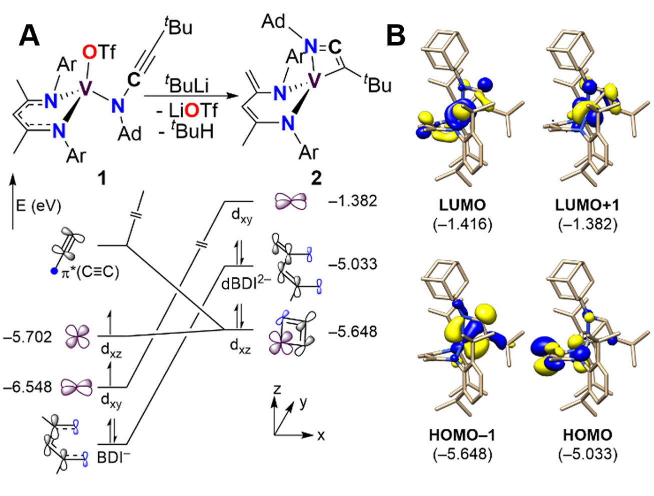

Figure 4. (A) Conceptual molecular orbitals during the interconversion between **1** and **2**. (B) DFT-calculated HOMO-1, HOMO, LUMO, and LUMO+1 of **2**.

nature of the transannular bond, complex **2** can be depicted as resonance form **2a** or **2b**, akin to dMCBDs.[11–12,14,16–17,19,21,41–44,46–47] However, one must also note that such scaffold could be redox non-innocent, and thus possess radical character. Furthermore, we found that the HOMO is dominated by the dBDI^{2-} contribution, which represents π-conjugation on the ligand backbone. This can be simply understood because deprotonation of BDI$^-$ to the dianionic dBDI^{2-} ligand increases the energy of the corresponding orbitals due to greater electrostatic repulsion.

To gain a better understanding on how the κ^2-azaalleneyl fragment in **2** forms, we turned our attention to a DFT-calculated reaction mechanism involving the conversion of **B** to **2** (Figure 5). Addition of C≡NAd to the vanadium alkylidyne complex **B** likely involves dissociative ligand exchange with diethyl ether and afford the isonitrile adduct intermediate **B1** located at −5.1 kcal/mol. Coordination of the carbon atom to V allows the lone-pair electrons of the isocyanide nitrogen moiety to traverse through transition state **B1-TS**, which involves a geometric reorientation of the isocyanide moiety to side-on. This transition state can be understood by converting the charge separated resonance form of the isocyanide moiety ($^-$C≡N$^+$–Ad) into the charge neutral form (C=N–Ad). Therefore, putative intermediate **B2**, which connects **B1** and the final product **2**, should be relevant in the mechanism as well since its transition state **B2-TS** mediates a [2+2]-cycloaddition between C≡NAd and the alkylidyne ligand. Despite significant efforts, we were unable to locate the transition state **B2-TS** due to the electron-deficient carbon atom in the isocyanide moiety, which violates the octet rule. As a result, the potential energy surfaces connecting **B2** and **B2-TS** are extremely shallow (see Supporting Information Figure S22 for details) and the final product **2** is likely formed without any appreciable reaction barrier, pushed forward by a large thermodynamic driving force of 46.1 kcal/mol. We propose that the reaction barrier from **B1** to **B2**, calculated to be 20.6 kcal/mol, is rate-determining, which is consistent with the reaction time and the experimental conditions.

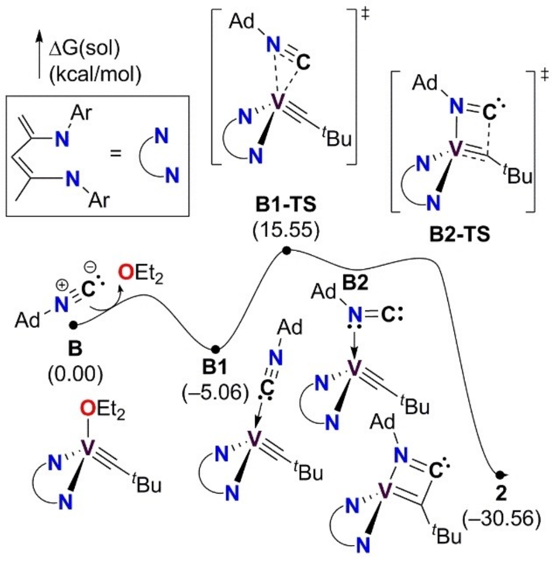

Figure 5. DFT-calculated reaction mechanism of the formation of complex **2** from **B**. Artificial curves connecting the optimized structures are utilized in the Figure for illustrative purposes only.

Two diamagnetic vanadium alkylidyne complexes, **A** and **B**, react with 1-adamantyl isonitrile, C≡NAd, to yield a paramagnetic ($S=1$) [V^{III}] κ^1-*N*-ynamide complex **1**, and a diamagnetic [V^{III}] κ^2-*C*,*N*-azaalleneyl complex, **2**, respectively. Brønsted acid-base chemistry allows the interconversion between the two, and this transformation is accompanied by the spin-state change of the [V^{III}] ion. These spin-state transformations in the HdMCBD may provide insights into how dMCBDs (Scheme 1, i and iii) might engage in polymerization of alkyne via the formation of a putative high-spin ring opened carbene species. We have shown how [(Ad)NCC(^{t}Bu)]$^-$ can bind to the vanadium center in a monodentate or a chelating fashion. Despite the [V^{III}] ion maintaining a relatively similar geometry in these two [(Ad)NCC(^{t}Bu)]$^-$ binding modes, the 3d orbital ordering of metal is significantly different, leading to a spin-state change between the two. Thus, by leveraging the ability for 3d^n, $n \geq 2$, transition metals to undergo facile spin-state transformations, we could envision developing catalytic systems that utilize this reversible spin-state transformation with the aid of Brønsted acid-base chemistry.

Supporting Information

The data that supports the findings of this study are available in the Supporting Information of this article.

Acknowledgements

D.J.M. thanks the University of Pennsylvania and the U. S. National Science Foundation (NSF; CHE-2154620) for financial support. M.-H.B. thanks the Institute for Basic Science in Korea for financial support (IBS-R010-A1). J.B.R. thanks the Vagelos Institute for Energy Science and Technology (VIEST) for a predoctoral fellowship. A portion of this work was performed at the National High Magnetic Field Laboratory, which is supported by NSF Cooperative Agreement No. DMR-1644779 and the State of Florida.

Conflict of Interest

The authors declare no conflict of interest.

Data Availability Statement

The data that support the findings of this study are available in the supplementary material of this article.

Keywords: Alkylidynes · Metallacycles · Ynamide · Azaalleneyl · Bent Allene

[1] M. Cui, G. Jia, *J. Am. Chem. Soc.* **2022**, *144*, 12546–12566.
[2] A. Fürstner, *Angew. Chem. Int. Ed.* **2013**, *52*, 2794–2819.
[3] H. Ehrhorn, M. Tamm, *Chem. Eur. J.* **2019**, *25*, 3190–3208.
[4] R. R. Schrock, *Angew. Chem. Int. Ed.* **2006**, *45*, 3748–3759.
[5] A. Fürstner, P. W. Davies, *Chem. Commun.* **2005**, 2307–2320.
[6] A. Fürstner, *Angew. Chem. Int. Ed.* **2013**, *52*, 2794–2819.
[7] K. C. Nicolaou, P. G. Bulger, D. Sarlah, *Angew. Chem. Int. Ed.* **2005**, *44*, 4490–4527.
[8] K. Jyothish, Q. Wang, W. Zhang, *Adv. Synth. Catal.* **2012**, *354*, 2073–2078.
[9] S. Lysenko, J. Volbeda, P. G. Jones, M. Tamm, *Angew. Chem. Int. Ed.* **2012**, *51*, 6757–6761.
[10] L. G. McCullough, R. R. Schrock, J. C. Dewan, J. C. Murdzek, *J. Am. Chem. Soc.* **1985**, *107*, 5987–5998.
[11] J. H. Wengrovius, J. Sancho, R. R. Schrock, *J. Am. Chem. Soc.* **1981**, *103*, 3932–3934.
[12] L. G. McCullough, M. L. Listemann, R. R. Schrock, M. R. Churchill, J. W. Ziller, *J. Am. Chem. Soc.* **1983**, *105*, 6729–6730.
[13] R. R. Schrock, J. H. Freudenberger, M. L. Listemann, L. G. McCullough, *J. Mol. Catal.* **1985**, *28*, 1–8.
[14] J. H. Freudenberger, R. R. Schrock, *Organometallics* **1986**, *5*, 1411–1417.
[15] H. Strutz, J. Dewan, R. Schrock, *J. Am. Chem. Soc.* **1985**, *107*, 5999–6005.
[16] M. R. Churchill, J. W. Ziller, *J. Organomet. Chem.* **1985**, *281*, 237–248.
[17] K. Weiss, R. Goller, G. Loessel, *J. Mol. Catal.* **1988**, *46*, 267–275.
[18] H. Ehrhorn, M. Tamm, *Chem. Eur. J.* **2019**, *25*, 3190–3208.
[19] J. Heppekausen, R. Stade, A. Kondoh, G. Seidel, R. Goddard, A. Fürstner, *Chem. Eur. J.* **2012**, *18*, 10281–10299.
[20] A. Bray, A. Mortreux, F. Petit, M. Petit, T. Szymanska-Buzar, *J. Chem. Soc. Chem. Commun.* **1993**, 197–199.
[21] M. G. Jafari, J. B. Russell, H. Lee, B. Pudasaini, D. Pal, Z. Miao, M. R. Gau, P. J. Carroll, B. S. Sumerlin, A. S. Veige, M.-H. Baik, D. J. Mindiola, *J. Am. Chem. Soc.* **2024**, *146 (5)*, 2997–3009.
[22] M. Cui, G. Jia, *J. Am. Chem. Soc.* **2022**, *144*, 12546–12566.
[23] R. Lhermet, A. Fürstner, *Chem. Eur. J.* **2014**, *20*, 13188–13193.
[24] O. Coutelier, A. Mortreux, *Adv. Synth. Catal.* **2006**, *348*, 2038–2042.
[25] B. Haberlag, M. Freytag, C. G. Daniliuc, P. G. Jones, M. Tamm, *Angew. Chem. Int. Ed.* **2012**, *51*, 13019–13022.
[26] O. Coutelier, G. Nowogrocki, J.-F. Paul, A. Mortreux, *Adv. Synth. Catal.* **2007**, *349*, 2259–2263.
[27] F. Reiß, M. Reiß, J. Bresien, A. Spannenberg, H. Jiao, W. Baumann, P. Arndt, T. Beweries, *Chem. Sci.* **2019**, *10*, 5319–5325.
[28] X. Shi, S. Li, M. Reiß, A. Spannenberg, T. Holtrichter-Rößmann, F. Reiß, T. Beweries, *Chem. Sci.* **2021**, *12*, 16074–16084.
[29] J. B. Russell, D. Konar, T. Keller, M. R. Gau, P. J. Carroll, J. Telser, D. W. Lester, A. S. Veige, B. S. Sumerlin, D. J. Mindiola, *Angew. Chem. Int. Ed.* **2024**, *63*, e202318956.
[30] J. J. Carbó, A. Martín, M. Mena, A. Pérez-Redondo, J.-M. Poblet, C. Yélamos, *Angew. Chem. Int. Ed.* **2007**, *46*, 3095–3098.
[31] C. Wang, W. Mao, L. Xiang, Y. Yang, J. Fang, L. Maron, X. Leng, Y. Chen, *Chem. Eur. J.* **2018**, *24*, 13903–13917.
[32] R. S. Drago, in *Physical Methods in Chemistry*, Surfside Scientific Publishers, Gainesville, **1992**, p. 476.
[33] P. L. W. Tregenna-Piggott, D. Spichiger, G. Carver, B. Frey, R. Meier, H. Weihe, J. A. Cowan, G. J. McIntyre, G. Zahn, A.-L. Barra, *Inorg. Chem.* **2004**, *43*, 8049–8060.
[34] J. G. Andino, U. J. Kilgore, M. Pink, A. Ozarowski, J. Krzystek, J. Telser, M.-H. Baik, D. J. Mindiola, *Chem. Sci.* **2010**, *1*, 351–356.
[35] B. L. Tran, J. Krzystek, A. Ozarowski, C. H. Chen, M. Pink, J. A. Karty, J. Telser, K. Meyer, D. J. Mindiola, *Eur. J. Inorg. Chem.* **2013**, *2013*, 3916–3929.
[36] L. N. Grant, J. Krzystek, B. Pinter, J. Telser, H. Grützmacher, D. J. Mindiola, *Chem. Commun.* **2019**, *55*, 5966–5969.
[37] D. Adhikari, F. Basuli, J. H. Orlando, X. Gao, J. C. Huffman, M. Pink, D. J. Mindiola, *Organometallics* **2009**, *28*, 4115–4125.
[38] M. Luo, L. Long, H. Zhang, Y. Yang, Y. Hua, G. Liu, Z. Lin, H. Xia, *J. Am. Chem. Soc.* **2017**, *139*, 1822–1825.
[39] J.-K. F. Buijink, J. H. Teuben, H. Kooijman, A. L. Spek, *Organometallics* **1994**, *13*, 2922–2924.
[40] B. Hessen, A. Meetsma, J. H. Teuben, *J. Am. Chem. Soc.* **1989**, *111*, 5977–5978.
[41] L. G. McCullough, R. R. Schrock, J. C. Dewan, J. C. Murdzek, *J. Am. Chem. Soc.* **1985**, *107*, 5987–5998.
[42] H. Ehrhorn, D. Bockfeld, M. Freytag, T. Bannenberg, C. E. Kefalidis, L. Maron, M. Tamm, *Organometallics* **2019**, *38*, 1627–1639.
[43] F. Reiß, M. Reiß, J. Bresien, A. Spannenberg, H. Jiao, W. Baumann, P. Arndt, T. Beweries, *Chem. Sci.* **2019**, *10*, 5319–5325.
[44] X. Shi, S. Li, M. Reiß, A. Spannenberg, T. Holtrichter-Rößmann, F. Reiß, T. Beweries, *Chem. Sci.* **2021**, *12*, 16074–16084.
[45] J. Peng, J. Zhao, Z. Hu, D. Liang, J. Huang, Q. Zhu, *Org. Lett.* **2012**, *14*, 4966–4969.
[46] R. R. Schrock, J. H. Freudenberger, M. L. Listemann, L. G. McCullough, *J. Mol. Catal.* **1985**, *28*, 1–8.
[47] H. Strutz, J. C. Dewan, R. R. Schrock, *J. Am. Chem. Soc.* **1985**, *107*, 5999–6005.
[48] J. C. Slater, *The self-consistent field for molecules and solids: quantum theory of molecules and solids*, McGraw-Hill Book Company, **1974**.
[49] S. H. Vosko, L. Wilk, M. Nusair, *Can. J. Phys.* **1980**, *58*, 1200–1211.
[50] A. D. Becke, *Phys. Rev. A* **1988**, *38*, 3098–3100.
[51] A. D. Becke, *J. Chem. Phys.* **1993**, *98*, 5648–5652.
[52] C. Lee, W. Yang, R. G. Parr, *Phys. Rev. B* **1988**, *37*, 785–789.
[53] S. Grimme, J. Antony, S. Ehrlich, H. Krieg, *J. Chem. Phys.* **2010**, *132*, 154104.
[54] T. H. Dunning, *J. Chem. Phys.* **1989**, *90*, 1007–1023.
[55] R. Ditchfield, W. J. Hehre, J. A. Pople, *J. Chem. Phys.* **1971**, *54*, 724–728.
[56] Deposition numbers 22262656 (for **1**), 22262655 (for **2**) (all structures are collected at 100 K) contain the supplementary crystallographic data for this paper. These data are provided free of charge by the joint Cambridge Crystallographic Data Centre and Fachinformationszentrum Karlsruhe Access Structures service.

Manuscript received: January 20, 2024
Accepted manuscript online: March 3, 2024
Version of record online: April 17, 2024